Restricted Phenyl Rotation in Pyridyl Thioether Ligands N,S-Chelated to Congested Diiminoruthenium Cores

Laura Baradello,[a] Sandra Lo Schiavo,[a] Francesco Nicolò,[a] Santo Lanza,[a] Giuseppe Alibrandi,[a] and Giuseppe Tresoldi*[a]

Keywords: Activation barriers / N,S ligands / Restricted rotation / Ruthenium

The thioethers 2-pyridylmethyl *p*-tolyl sulfide (**a**) and *p*-chlorophenyl 2-pyridylmethyl sulfide (**b**) react with the precursors *cis*-[$RuCl_2$(*N*,*N*-diimine)$_2$] [diimine = di-2-pyridyl sulfide (dps), **1**; 2,2′-bis(4-methylpyridyl) sulfide (4mdps), **2**; 2,2′-bis(5-methylpyridyl) sulfide (5mdps), **3**; di-2-pyrimidyl sulfide (dprs), **4**; and 2,2′-bis(5-ethylpyrimidyl) sulfide (5edprs), **5**] in the presence of NH_4PF_6 to give the complexes [Ru(*N*,*N*-diimine)$_2$(*N*,*S*-**a**)][PF_6]$_2$ and [Ru(*N*,*N*-diimine)$_2$(*N*,*S*-**b**)][PF_6]$_2$, respectively. As a consequence of the *N*,*S* chelation all the complexes contain a five-membered RuSCCN(*Ru*–*N*) ring, the sulfur and ruthenium atoms of which are stereogenic centres, with (*R*) and (*S*) and Δ and Λ configurations, respectively. Furthermore, the coordinated thioethers contain anisochronous methylene protons and phenyl protons which are sensor nuclei for pyramidal sulfur inversion and rotation of the pendant phenyl ring, respectively. In the low-temperature ^{1}H NMR spectra of the complexes a single AB system for the methylene protons, in agreement with a fast sulfur inversion, is observed. Well-separated signals of the two *ortho*- as well as the *meta*-phenyl protons, indicating restricted phenyl rotation, are also observed. At higher temperatures the fast exchange of the two halves of the phenyl ring leads to averaged signals for the phenyl protons. The rates and activation energies of this fluxional process were measured by one-dimensional band-shape analysis. Certain trends were immediately apparent. The rotation barrier values ($\Delta G^{\#}_{298}$) of the dps, 4mdps and 5mdps complexes were ca. 4.0 kJ·mol^{-1} lower than those of the dprs and 5edprs complexes. On the contrary, substitution of H^4 or H^5 dps protons with methyl groups and H^5 dprs protons with ethyl groups, as well as substitution of **a** with **b**, leaves the rotation-barrier values practically unchanged. This effect can be correlated to the steric hindrance produced by the two ligands *cis* to the rotating group. The crystal structure of the enantiomeric couple Δ*S*/Λ*R* of [Ru(dps)$_2$(2-pyridymethyl 2-pyridyl sulfide)][PF_6]$_2$ (**1c**), in which the 2-pyrimidylmethyl 2-pyridyl sulfide (**c**) ligand acts in an *N*,*S*-bidentate mode forming a five-membered RuSCCN(*Ru*–*N*) chelate ring, is also reported.

Introduction

The chemistry of di-2-pyridyl sulfide (dps) is of interest in that the ligand, which usually adopts an *N*,*N*-bidentate coordination,[1−13] can exhibit a variety of bonding modes to metal atoms, for example monodentate,[10−12] and bridging.[11−14] Consequently, dps complexes can exhibit interconversion between different coordination species or fluxional processes.[10−12] The *N*,*N* chelation[15−20] of dps, and similar thioether compounds containing heterocycles, to the ruthenium(II) ion, and a *cis* arrangement[15−17,19,20] around the metal atom, are usually observed, although complexes with a *trans* configuration[18] or which contain a four-membered RuSCN(*Ru*−*N*)[19] ring have also been obtained. As a consequence of the *N*,*S* coordination, the thioether ligand contains a stereogenic sulfur centre [(*R*) and (*S*) configurations] and a pendant ring. The ^{1}H and ^{13}C NMR spectra of the complexes containing *cis*-Ru(*N*,*N*-dprs)$_2$ or *cis*-Ru(*N*,*N*-dps)$_2$ fragments (dprs = di-2-pyrimidyl sulfide) and the *N*,*S*-chelated thioether ligand phpys (phenyl pyridyl sulfide) below 240 K are temperature-dependent due to the restricted rotation of the pendant ring.

The NMR investigation of [Ru(*N*,*N*-diimine)$_2$(*N*,*S*-thioether)][PF_6]$_2$ [20] (diimine = dps or dprs; thioether = pySCH_2R or prSCH_2R, where py = pyridyl, pr = pyrimidyl and R = phenyl derivative) shows the presence of two invertomers as pairs of enantiomers (Δ*R*, Λ*S* and Δ*S*, Λ*R*) due to the Δ and Λ configurations of the ruthenium atom and the (*R*) and (*S*) configurations of the sulfur atom. The sulfur inversion produces the exchange [(*R*) ⇄ (*S*)] whereas the racemization process (Δ ⇄ Λ) was absent and the rotation of the pendant ring fast.

In order to study the effect of the steric hindrance of the Ru(diimine)$_2$ fragment on the phenyl rotation and the effect of the ring size on the sulfur inversion we have selected a series of [$RuCl_2$(diimine)$_2$] precursors and thioethers suitable for *N*,*S* chelation. We report on the dynamic behaviour

[a] Dipartimento di Chimica Inorganica, Chimica Analitica e Chimica Fisica, Università di Messina,
Salita Sperone 31, 98166 Messina, Italy
Fax: + 39-090-393756
E-mail: Tresoldi@chem.unime.it

  DOI: 10.1002/ejic.200400120

of the compounds obtained from 2-pyridylmethyl *p*-tolyl sulfide (**a**) and *p*-chlorophenyl 2-pyridylmethyl sulfide (**b**) with *cis*-[$RuCl_2$(*N*,*N*-diimine)$_2$] compounds [diimine = dps, **1**; 2,2′-bis(4-methylpyridyl) sulfide (4mdps), **2**; 2,2′-bis(5-methylpyridyl) sulfide (5mdps), **3**; dprs, **4** and 2,2′-bis(5-ethylpyrimidyl) sulfide (5edprs) **5**]. The crystal structure of the couple $\Delta S/\Lambda R$ of [Ru(dps)$_2$(2-pyridymethyl 2-pyridyl sulfide)][PF_6]$_2$ (**1c**) is also reported.

Results

Synthesis of the Compounds Containing an N,S-Chelate Ligand

The air-stable compounds **1a**, **3a**−**5a**, **1b**−**5b** and **1c** were obtained by the reactions depicted in Scheme 1. The new precursors [$RuCl_2$(*N*,*N*-4mdps)$_2$] (**2**), [$RuCl_2$(*N*,*N*-5mdps)$_2$] (**3**) and [$RuCl_2$(*N*,*N*-5edprs)$_2$] (**5**) were prepared from $RuCl_3 \cdot 3H_2O$ and 4mdps,[21] 5mdps[21] or the new ligand 5edprs; see Exp. Sect.).

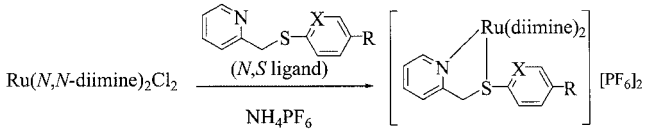

	Ru(*N*,*N*-diimine)$_2$Cl$_2$	*N*,*S* ligand	Complex
1	Ru(dps)$_2$Cl$_2$	**a** (X = CH, R = Me)	**1a**
3	Ru(5mdps)$_2$Cl$_2$	**a**	**3a**
4	Ru(dprs)$_2$Cl$_2$	**a**	**4a**
5	Ru(5edprs)$_2$Cl$_2$	**a**	**5a**
1	Ru(dps)$_2$Cl$_2$	**b** (X = CH, R = Cl)	**1b**
2	Ru(4mdps)$_2$Cl$_2$	**b**	**2b**
3	Ru(5mdps)$_2$Cl$_2$	**b**	**3b**
4	Ru(5edprs)$_2$Cl$_2$	**b**	**4b**
5	Ru(dps)$_2$Cl$_2$	**c** (X = N, R = H)	**1c**

Scheme 1

The complexes are yellow or orange solids that are soluble in acetone or acetonitrile and slightly soluble in methanol, ethanol and water. They were characterised by elemental analysis, conductivity measurements in acetonitrile solution with values characteristic of 1:2 electrolytes (330−300 $S \cdot cm^2 \cdot mol^{-1}$), IR spectroscopy, which shows the bands of PF_6^- (ca. 842 and 558 cm^{-1}) and those characteristic of thioether ligands in the range 1630−1540 cm^{-1}. This indicates that the ligands dps, 4mdps, 5mdps, dprs and 5edprs act as bidentate *N*,*N*-chelate ligands,[8−20] whereas **a**, **b** and **c** are *N*,*S*-chelate ligands.[19,20] These findings were confirmed by subsequent ^1H and ^{13}C NMR spectroscopic studies.

Low-Temperature ^1H NMR Spectra

At low temperatures the NMR spectra of these complexes show well-separated signals of the two *ortho*- (as well as the *meta*-) phenyl protons. The spectrum of **4b** at 218 K in the δ = 8.2−3.7 ppm range is shown in Figure 1; the data are listed in Table 1. Because of the slow phenyl rotation two doublets of doublets are observed in the phenyl region for the *ortho*-protons at δ = 8.09 (partially overlapped with the signal of the H^5 pyrimidine proton) and 5.38 ppm, labelled **M** and **N**, respectively. Furthermore, two doublets of doublets for the *meta*-protons are observed at δ = 7.60 and 6.75 ppm, labelled **O** and **P**, respectively. The coupling constants between **M** and **O** and **N** and **P** are 8.6 Hz and between **M** and **N** and **O** and **P** 2.3 Hz. In the methylene region two doublets appear at δ = 4.65 and 3.87 ppm ($^2J_{H,H}$ = 17.4 Hz).

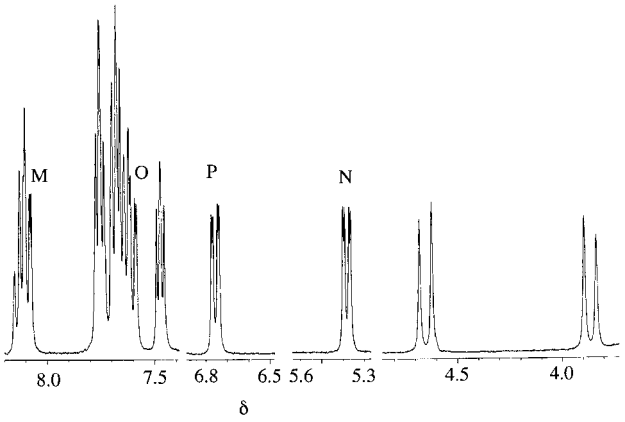

Figure 1. ^1H NMR spectrum of [Ru(*N*,*N*-dprs)$_2$(*N*,*S*-**b**)][PF_6]$_2$ (**4b**) at 218 K in $(CD_3)_2CO$ (range δ = 8.2−3.7 ppm)

The full assignment of the signals and the solution structure was based on 2D COSY, phase-sensitive 2D NOESY, decoupling experiments and one-dimensional ^1H NMR spectra at variable temperatures. In this way the twelve signals, as doublets of doublets due to the protons of the four pyrimidine rings with the coupling constants $J_{4,5} \approx 4.6$, $J_{4,6} \approx 2.1$, $J_{5,6} \approx 6.0$ Hz and the ten signals due to the protons of the pyridine, the phenyl and methylene groups of the **b** ligand, were assigned.

Dynamic NMR Studies

The dynamic behaviour of the complexes was preliminarily examined by phase-sensitive 2D NOESY spectroscopy, which shows the interchanges (positive cross-peaks) and the interactions (negative cross-peaks) between the protons. The phase-sensitive 2D NOESY spectra of the dprs and 5edprs complexes were recorded almost at the same temperature (245−250 K) whereas those of the dps, 4mdps and 5mdps complexes were recorded at lower temperatures as the dynamic process is faster than for the dprs and 5edprs complexes (vide infra).

The spectrum for **4b**, at 248 K, is shown in Figure 2. At this temperature the *ortho*-phenyl signals as well as the *meta* signals are split as the fluxional process that exchanges the two halves of the phenyl ring is slow. Positive cross-peaks, due to chemical exchange of magnetization, are detected between the phenyl protons **M** and **N** (at δ = 8.09 and 5.38

Table 1. Low-temperature ^{1}H NMR spectroscopic data

Complex[a]	*N,S*-ligand positions						*N,N*-ligand positions				
T [K]	2	3	4	5	6	CH_2	ring	3	4	5	6
1a		7.60[b]	7.84[b]	7.58[b]	9.40[b]	4.38[b]	C	7.62	8.14	7.63	9.35
218	7.80[c]	7.29[c]	2.12[d]	6.38[c]	5.07[c]	3.60[b]	D	8.19	8.03	7.17	7.60
	$J_{2,3} = J_{5,6} = 7.7$			$J_{2,6} = J_{3,5} = 1.7$		$J = 16.7$	E	8.16	8.23	7.36	8.03
							F	7.62	8.11	7.64	9.16
3a		7.56[b]	8.03[b]	7.63[b]	9.49[b]	4.28[b]	C	7.38	7.76	2.35[e]	9.24
213	7.76[c]	7.28[c]	2.11[d]	6.40[c]	5.04[c]	3.48[b]	D	7.88	7.84	1.89[e]	7.84
	$J_{2,3} = J_{5,6} = 8.2$			$J_{2,6} = J_{3,5} = 1.8$		$J = 16.9$	E	8.09	8.01	2.03[e]	7.92
							F	7.67	8.01	2.35[e]	8.99
4a		7.68[b]	8.12[b]	7.75[b]	9.40[b]	4.52[b]	C		8.54	7.60	9.42
223	7.90[c]	7.34[c]	2.14[d]	6.49[c]	5.10[c]	3.79[b]	D		8.97	7.45	8.79
	$J_{2,3} = J_{5,6} = 8.2$			$J_{2,6} = J_{3,5} = 2.1$		$J = 17.5$	E		9.13	7.65	9.04
							F		8.93	7.74	9.63
5a		7.65[b]	8.10[b]	7.73[b]	9.51[b]	4.47[b]	C	1.07[e]	8.52	2.66[f]	9.36
228	7.87[c]	7.33[c]	2.14[d]	6.48[c]	4.97[c]	3.77[b]	D	0.85[e]	8.95	2.34[f]	8.74
	$J_{2,3} = J_{5,6} = 8.0$			$J_{2,6} = J_{3,5} = 2.2$		$J = 17.2$	E	0.92[e]	9.07	2.41[f]	8.92
							F	1.14[e]	8.91	2.69[f]	9.62
1b		7.61[b]	8.08[b]	7.65[b]	9.38[b]	4.50[b]	C	7.57	7.89	7.59	9.43
208	7.98[c]	7.58[c]		6.73[c]	5.26[c]	3.67[b]	D	8.26	8.04	7.18	7.60
	$J_{2,3} = J_{5,6} = 8.5$			$J_{2,6} = J_{3,5} = 1.8$		$J = 16.9$	E	8.16	8.22	7.37	8.07
							F	7.60	8.03	7.58	9.18
2b		7.62[b]	8.00[b]	7.58[b]	9.29[b]	4.49[b]	C	7.46	2.28[e]	7.36	9.15
207	7.95[c]	7.56[c]		6.79[c]	5.18[c]	3.66[b]	D	8.05	2.39[e]	7.02	7.46
	$J_{2,3} = J_{5,6} = 8.6$			$J_{2,6} = J_{3,5} = 2.4$		$J = 17.0$	E	8.12	2.47[e]	7.22	8.05
							F	7.90	2.43[e]	7.49	8.96
3b		7.57[b]	8.02[b]	7.64[b]	9.48[b]	4.40[b]	C	7.48	7.84	2.33[e]	9.25
217	7.94[c]	7.54[c]		6.71[c]	5.25[c]	3.55[b]	D	8.04	7.93	1.89[e]	7.48
	$J_{2,3} = J_{5,6} = 8.5$			$J_{2,6} = J_{3,5} = 2.1$		$J = 16.9$	E	8.09	8.04	2.01[e]	7.89
							F	7.88	8.04	2.31[e]	8.99
4b		7.63[b]	8.13[b]	7.75[b]	9.41[b]	4.65[b]	C		8.61	7.67	9.46
218	8.09[c]	7.60[c]		6.75[c]	5.38[c]	3.87[b]	D		8.98	7.47	8.81
	$J_{2,3} = J_{5,6} = 8.6$			$J_{2,6} = J_{3,5} = 2.3$		$J = 17.4$	E		9.14	7.67	9.05
							F		8.94	7.75	9.66
5b		7.63[b]	8.08[b]	7.71[b]	9.49[b]	4.57[b]	C	1.07[e]	8.60	2.68[f]	9.35
218	8.04[c]	7.58[c]		6.73[c]	5.25[c]	3.81[b]	D	0.91[e]	8.92	2.31[f]	8.72
	$J_{2,3} = J_{5,6} = 8.6$			$J_{2,6} = J_{3,5} = 2.5$		$J = 17.4$	E	0.84[e]	9.07	2.40[f]	8.91
							F	1.37[e]	8.90	2.68[f]	9.61
1c		7.40[b]	7.72[b]	7.43[b]	9.25[b]	4.55[b]	C	7.50	7.90	7.49	9.15
223		7.93[g]	7.82[g]	7.19[g]	7.48[g]	3.69[b]	D	8.17	8.02	7.17	7.58
						$J = 16.9$	E	8.23	8.16	7.34	8.03
							F	8.00	8.09	7.62	9.17

[a] At 300.13 MHz, in [D$_6$]acetone; δ in ppm with respect to TMS, *J* in Hz. [b] Picolyl fragment. [c] Phenyl fragment. [d] Methyl of **a**. [e] Methyl of the *N,N* ligand. [f] Methylene of 5edprs. [g] Pyridyl fragment.

ppm, respectively) and **O** and **P** (at $\delta = 7.60$ and 6.75 ppm, respectively) while the strong NOEs (negative cross peaks) include interactions between the methylene protons, intra-ring interactions in the phenyl ring (**M/O** and **N/P**) and in the pyrimidine ring (H^6/H^5) and, most significantly, the following interactions: methylene proton at $\delta = 4.65$ ppm/H^3 pyridine proton at $\delta = 7.63$ ppm, methylene proton at $\delta = 3.87$ ppm/H^6 pyrimidine proton at $\delta = 9.66$ ppm, H^6 pyrimidine proton at $\delta = 9.46$ ppm/H^6 pyridine proton at $\delta = 9.41$ ppm, H^6 pyrimidine proton at $\delta = 9.46$ ppm and that at $\delta = 9.05$ ppm, H^6 pyrimidine proton at $\delta = 9.66$ ppm and that at $\delta = 8.81$ ppm. If we assume that the sulfur inversion is fast at low temperatures and that the phenyl rotation is slow, the *ortho*-phenyl protons (**M** and **N**) are anisochronous as are the *meta*-protons (**O** and **P**), and the phenyl rotation exchanges protons **M** and **N** and **O** and **P**. Furthermore the negative cross-peaks found in the 2D NOESY spectrum suggest that in the invertomer depicted (Figure 3) the pyrimidine ring labelled C is *cis* to the phenyl ring B and the ring F is *cis* to the pyridine ring A, while ring E is *trans* to the sulfur atom. In the other invertomer (not shown) the phenyl ring should be *cis* to the ring F.

Similar structures for the other complexes at low temperature can be deduced from the data listed in Table 1. The ring and the position of the protons were assigned by the one- and two-dimensional experiments mentioned previously and by comparison of the spectra. In particular, the solution structure depicted in Figure 4 is proposed for an invertomer of **1a**.

Upon warming the solutions, the spectral lines of the phenyl protons broaden and coalesce in the range 255−295 K. At 330 K, the highest temperature reached, averaged signals are observed for the *ortho*- as well the *meta*-phenyl protons of all the complexes (Table 2). For instance,

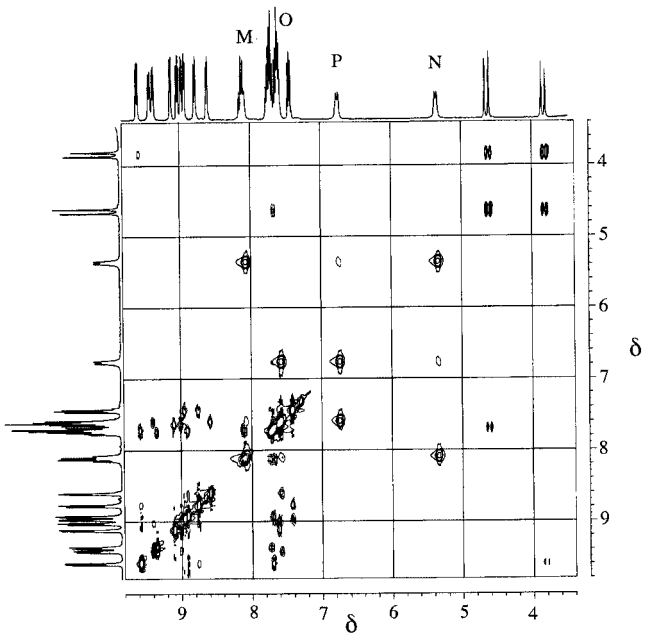

Figure 2. Phase-sensitive 2D NOESY spectrum of **4b** at 248 K in $(CD_3)_2CO$ (range δ = 9.8−3.4 ppm)

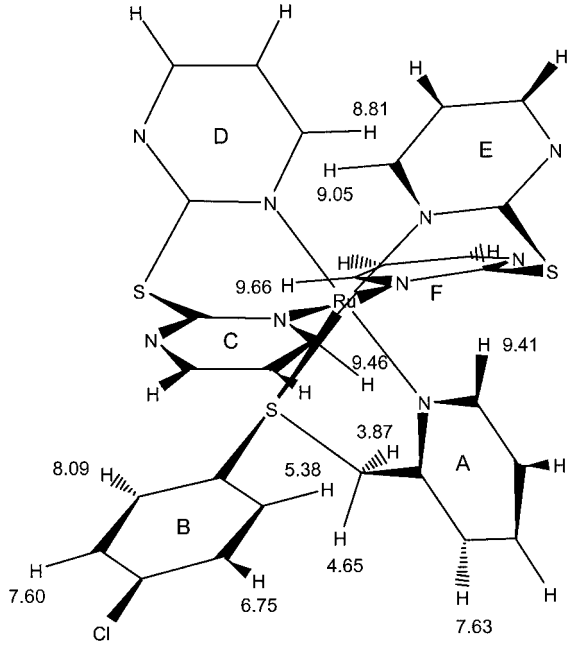

Figure 3. Proposed solution structure of **4b**; the rings are labelled A−F; the following signal assignments, based on 2D NOESY spectra at low temperatures, show vicinal protons at δ = 8.09−7.60, 6.75−5.38, 7.63−4.65, 9.66−3.87, 9.46−9.41, 9.46−9.05, 9.66−8.81 ppm

the *meta*- and the *ortho*-phenyl proton signals of **1a** are observed at δ = 6.83 and 6.50 ppm, respectively, near the statistical average of δ = 6.84 and 6.44 ppm, respectively, as expected for a single dynamic process. Furthermore, the *meta*- and the *ortho*-phenyl proton signals of **4b** are observed at δ = 7.12 and 6.67 ppm, respectively. The last signal in this complex, as well as in other dprs and 5edprs

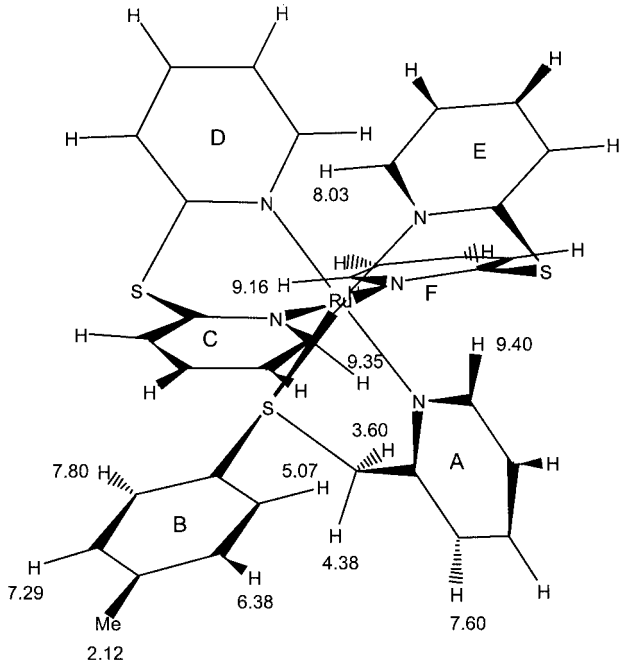

Figure 4. Proposed solution structure of **1a**; the rings are labelled A−F; the following signal assignments, based on 2D NOESY spectra at low temperatures, show vicinal protons at δ = 7.80−7.29, 6.38−5.07, 7.60−4.38, 9.16−3.60, 9.40−9.35, 6.38−2.12, 7.29−2.12, 9.40−8.03 ppm

complexes, is rather broad due to the great chemical-shift differences of the exchanging protons (ca. 2.7 ppm) and the energy-barrier values ($\Delta G^{\#}_{298} \approx$ 54.3 kJ·mol^{-1}, vide infra and Table 3). Although the dynamic behaviour of the complexes in CD_3CN parallels that observed in acetone, decomposition above 340 K is observed. Furthermore solubility problems in other solvents prevent detailed NMR studies at higher temperatures. It is worth noting that this process has a negligible effect on the methylene protons which appear, at all the temperatures, as a single AB system.

COSY and NOESY experiments were also performed at high temperatures allowing the complete assignment of the proton signals. In particular the signals of **4b** at δ = 9.20, 7.71, 8.06 and 7.64 ppm were assigned to the pyridine protons H^6, H^5, H^4 and H^3, respectively, of the *N*,*S*-coordinated ligand (Table 2).

The rates of the process were deduced by band-shape analysis of the phenyl signals. Some experimental and computer-simulated spectra are shown in Figure 5. Activation energy data were calculated from fifteen independent fittings in the temperature range 210−330 K. The activation energy data for the other complexes were obtained by a similar method and are collected in Table 3.

The ^{13}C NMR spectra of the complexes were interpreted easily, at least for the carbon signals of the *N*,*S*-chelate ligand, by comparison of the spectra of the present complexes with those of the free ligands and other complexes containing *N*,*S*-chelate ligands,[19,20] with the help of the jmod pulse sequence. The variable-temperature ^{13}C NMR spectra of **4b** in the range δ = 142−124 ppm are shown in

Table 2. ^{1}H NMR spectroscopic data

Complex[a]	*N*,*S*-ligand positions					*N*,*N*-ligand positions				
	3	4	5	6	CH_2	ring	3	4	5	6
a	7.37[b]	7.67[b]	7.19[b]	8.46[b]	4.24[b]					
	7.08[c]	7.25[d]	2.26[e]							
b	7.36[b]	7.68[b]	7.20[b]	8.45[b]	4.31[b]					
	7.06[c]	7.41[d]								
c	7.49[b]	7.67[b]	7.19[b]	8.48[b]	4.60[b]					
	7.28[f]	7.59[f]	7.07[f]	8.44[f]						
1a[g]	7.64[b]	7.98[b]	7.60[b]	9.23[b]	4.34[b]	C	7.97	8.08	7.56	9.10
	6.50[c]	6.83[d]	2.17[e]		3.59[b]	D	8.09	7.99	7.15	7.39
					J = 16.9	E	8.16	8.17	7.34	7.85
						F	7.49	7.83	7.56	9.30
3a[g]	7.55[b]	7.95[b]	7.65[b]	9.30[b]	4.29[b]	C	7.34	7.66	2.36[e]	9.12
	6.50[c]	6.83[d]	2.17[e]		3.60[b]	D	7.95	7.82	1.90[e]	7.03
					J = 16.9	E	8.04	7.96	2.03[e]	7.65
						F	7.85	7.92	2.35[e]	8.88
4a[g]	7.67[b]	8.09[b]	7.74[b]	9.23[b]	4.46[b]	C		8.51	7.51	9.28
	6.50[c]	6.93[d]	2.19[e]		3.70[b]	D		8.92	7.37	8.63
					J = 17.4	E		9.05	7.54	8.91
						F		8.87	7.65	9.40
5a[g]	7.63[b]	8.08[b]	7.77[b]	9.32[b]	4.40[b]	C	1.16[e]	8.45	2.74[h]	9.11
	6.48[c]	6.92[d]	2.20[e]		3.63[b]	D	1.03[e]	8.96	2.49[h]	8.75
					J = 17.3	E	0.96[e]	8.85	2.43[h]	8.45
						F	1.23[e]	8.80	2.78[h]	9.23
1b[g]	7.64[b]	7.98[b]	7.61[b]	9.23[b]	4.42[b]	C	7.58	7.87	7.58	9.31
	6.65[c]	7.06[d]			3.64[b]	D	8.09	7.99	7.15	7.38
					J = 17.0	E	8.17	8.15	7.34	7.84
						F	7.97	8.08	7.58	9.09
2b[g]	7.60[b]	7.97[b]	7.58[b]	9.15[b]	4.39[b]	C	7.39	2.34[e]	7.40	9.04
	6.63[c]	7.07[d]			3.63[b]	D	7.93	2.41[e]	6.98	7.12
					J = 17.0	E	7.99	2.50[e]	7.16	7.60
						F	7.80	2.47[e]	7.42	8.85
3b[g]	7.56[b]	7.97[b]	7.65[b]	9.31[b]	4.37[b]	C	7.45	7.71	2.38[e]	9.15
	6.66[c]	7.06[d]			3.64[b]	D	7.97	7.83	1.90[e]	7.03
					J = 16.9	E	8.05	7.97	2.02[e]	7.67
						F	7.85	7.92	2.35[e]	8.87
4b[g]	7.64[b]	8.06[b]	7.71[b]	9.20[b]	4.52[b]	C		8.53	7.51	9.26
	6.67[c]	7.12[d]			3.71[b]	D		8.89	7.34	8.60
					J = 17.5	E		9.02	7.51	8.87
						F		8.84	7.61	9.36
5b[g]	7.64[b]	8.08[b]	7.76[b]	9.34[b]	4.49[b]	C	1.15[e]	8.52	2.73[h]	9.15
	6.65[c]	7.14[d]			3.68[b]	D	1.02[e]	8.98	2.49[h]	8.78
					J = 17.4	E	0.94[e]	8.87	2.43[h]	8.50
						F	1.21[e]	8.80	2.76[h]	9.26
1c[g]	7.48[b]	7.89[b]	7.52[b]	9.05[b]	4.47[b]	C	7.40	7.75	7.42	9.18
	7.90[f]	7.80[f]	7.16[f]	7.40[f]	3.66[b]	D	8.10	8.00	7.18	7.59
					J = 16.7	E	8.10	8.16	7.33	7.83
						F	7.90	8.08	7.57	9.09

[a] At 300.13 MHz, in [D_6]acetone, at 298 K unless stated otherwise; δ in ppm with respect to TMS, J in Hz. [b] Picolyl fragment. [c] *ortho*-Phenyl proton. [d] *meta*-Phenyl proton. [e] Methyl proton. [f] Pyridyl fragment. [g] At 330 K. [h] Methylene of 5edprs.

Figure 6. In the ^{13}C NMR spectrum at 208 K the signals of the more deshielded carbon atoms appear at δ = 169.5, 169.2, 168.9 and 168.3 ppm (quaternary pyrimidine carbon atoms), while two overlapped signals for the C^6 pyrimidine carbon atoms appear at δ = 164.6 ppm, the others being well separated (δ = 164.5 and 163.0 ppm). The signal of the more deshielded carbon atom of **b** is observed at δ = 162.40 ppm (quaternary pyridine carbon atoms) while the C^6 pyridine carbon atom (δ = 155.5 ppm) is shielded with respect to the C^4 pyrimidine carbon atoms (δ = 158.6, 158.2, 158.1 and 156.8 ppm). Figure 6 shows the C^4 pyridine signal (δ = 138.6 ppm), the *ortho*-phenyl carbon signals (δ = 135.6 and 128.5 ppm), the *meta*-phenyl carbon signals (δ = 129.4 and 129.3 ppm), the CS signal (δ = 135.5 ppm), the CCl signal (δ = 128.5 ppm) and the signals of the C^3 and C^5 pyridine carbon atoms of **b** at δ = 124.3 and 124.1 ppm. The signals of the C^5 pyrimidine carbon atoms (not shown in Figure 6) are observed at δ = 122.2, 121.6 ppm, with two overlapping signals at δ = 121.3 ppm.

Upon warming the solutions, the signals of the *ortho*- and *meta*-phenyl carbon atoms broadened and then coalesced. The coalescence temperature (T_c) for the *meta*-phe-

Table 3. Activation energy data

	$\Delta G^{\#}_{298}$ [kJ·mol^{-1}]	$\Delta H^{\#}$ [kJ·mol^{-1}]	$\Delta S^{\#}$ [J·K^{-1}·mol^{-1}]
1a	50.0 ± 0.2	43.9 ± 1.2	−20.6 ± 4.9
1b	49.7 ± 0.1	50.5 ± 0.7	+2.8 ± 2.7
2b	50.1 ± 0.2	55.4 ± 1.8	+17.6 ± 6.6
3a	49.1 ± 0.1	50.7 ± 1.1	+5.4 ± 4.0
3b	49.7 ± 0.1	55.1 ± 1.0	+18.0 ± 3.5
4a	53.5 ± 0.2	49.6 ± 2.0	−13.0 ± 7.5
4b	54.3 ± 0.1	60.5 ± 1.1	+20.8 ± 4.2
5a	55.4 ± 0.6	73.6 ± 2.8	+61.1 ± 9.6
5b	55.2 ± 0.1	61.6 ± 0.7	+21.4 ± 2.5

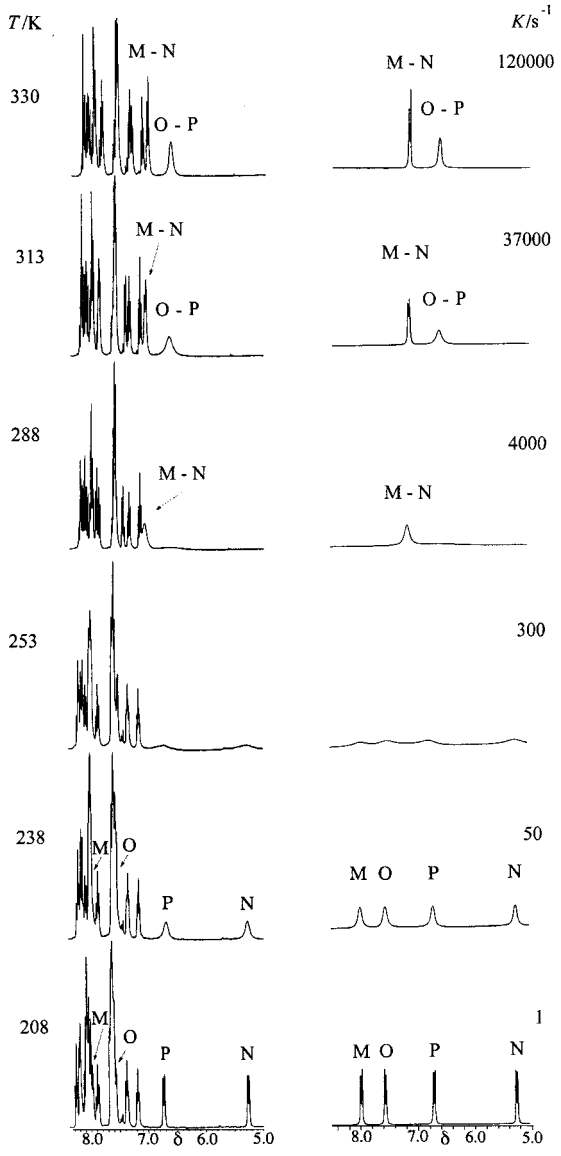

Figure 5. Selected variable-temperature ^{1}H NMR spectra of [Ru(*N*,*N*-dps)$_2$(*N*,*S*-**b**)][PF$_6$]$_2$ (**1b**) in (CD$_3$)$_2$CO (range δ = 8.4−4.8 ppm); simulated spectra on the right

nyl carbon atoms is 255 K. Their chemical-shift difference at 208 K is 12.09 Hz. The value of $\Delta G^{\#}_{255}$ (55.2 kJ·mol^{-1}), calculated from $\Delta G^{\#}_{T_c}$ = 19.14 T_c 10^{-3} (9.97 + logT_c/$\Delta\nu$),

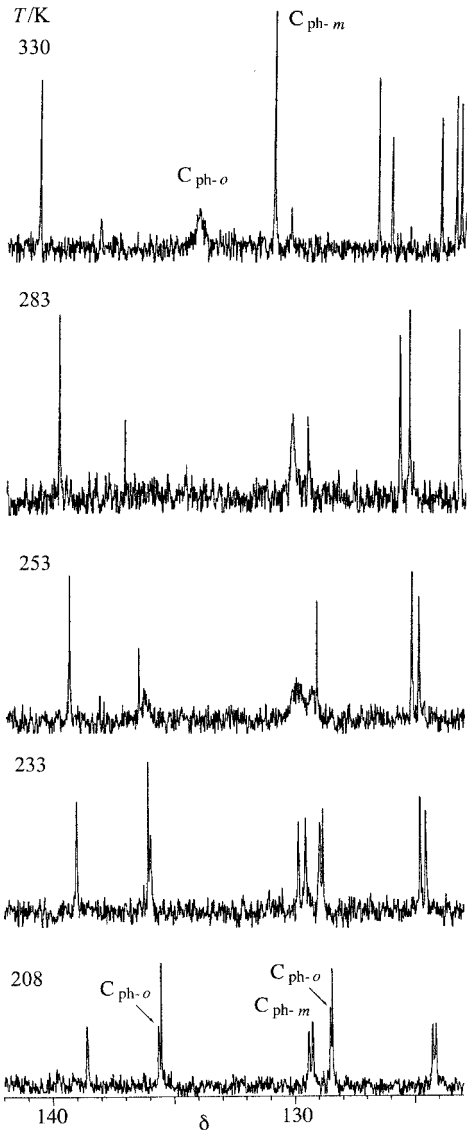

Figure 6. Selected variable-temperature ^{13}C NMR spectra of **4b** in (CD$_3$)$_2$CO (range δ = 141−124 ppm)

is in good agreement with the activation-energy barriers ($\Delta H^{\#}$ = 60.5 kJ·mol^{-1} and $\Delta S^{\#}$ = 20.8 J·K^{-1}·mol^{-1}) listed in Table 3.

In the fast-exchange regime (330 K) averaged signals of the *ortho*-phenyl (δ = 134.1 ppm) and *meta*-phenyl carbon atoms (δ = 131.0 ppm) are observed. Selected ^{13}C NMR spectroscopic data at low and high temperatures are listed in Table 4.

Molecular Structure of [Ru(dps)$_2$(2-pyridyl 2-pyridylmethyl sulfide)][PF$_6$]$_2$·(CH$_3$)$_2$CO (1c·C$_3$H$_6$O)

The complex cation of Ru^{2+} crystallizes in a 1:2 ratio with the hexafluorophosphate anions (both affected by a noticeable rotational disorder) for charge balance and in a 1:1 ratio with a disordered acetone molecule of the solvent. The crystal packing is stabilized by several hydrogen-bond interactions involving the fluorine atoms of the PF_6^-

Table 4. Selected ^{13}C NMR spectroscopic data[a]

Complex	T [K]	*N,S* ligand										
		Pyridyl ring							Other signals			
		C−CH_2	C^3	C^4	C^5	C^6	C^{ortho}	C^{meta}	CH_2	C−S	C−CH_3	CH_3
1a	228	163.2	124.2	139.2	124.1	156.1	132.1	130.0	46.7	140.8	127.6	20.0
		158.4[b]	157.5[b]	157.5[b]	157.2[b]		127.4	129.6				
	318	164.5	125.6	140.6	125.3	157.3	132.1	131.0	48.3	142.4	129.0	21.2
		159.0[b]	158.7[b]	158.5[b]	158.4[b]							
3a	218	162.8	123.5	137.7	123.4	154.8	131.4	129.8	46.2	140.1	127.6	19.7
		157.1[b]	156.9[b]	156.2[b]	156.1[b]		127.5	128.8	16.5[c]	16.3[c]	16.0[c]	16.0[c]
	328	163.0	123.7	137.8	123.7	154.8	130.4	129.2	49.2	140.5		20.0
		156.4[b]	156.2[b]	155.6[b]	154.9[b]				16.5[c]	16.3[c]	16.1[c]	16.0[c]
4a	228	163.5	125.1	139.3	124.9	156.3	134.1	130.0	46.7	141.5	126.8	20.2
		165.4[b]	165.4[b]	165.3[b]	163.4[b]		132.0	129.2				
	318	164.6	126.4	140.4	125.9	157.5	132.8	131.4	48.2	142.9	127.8	21.1
		166.3[b]	166.2[b]	166.2[b]	164.5[b]							
5a	228	163.9	124.3	138.7	124.0	156.0	133.9	130.3	46.1[d]	140.9	126.5	19.7
		167.6[b]	167.0[b]	166.9[b]	166.0[b]		127.2	129.2	15.5[c]	15.5[c]	15.1[c]	15.0[c]
	329	165.0	126.6	140.8	126.3	158.3	132.5	131.8	48.8[e]	143.4		21.5
		165.2[b]	165.2[b]	165.0[b]	164.9[b]				16.3[c]	16.1[c]	15.6[c]	15.5[c]
1b	228	162.6	124.1	138.2	124.0	155.4	135.4	129.7	46.2	135.6	127.8[f]	
		157.8[b]	157.2[b]	156.9[b]	156.0[b]		128.9	129.3				
	328	164.1	125.8	139.8	125.5	157.6	133.9	131.0	48.2	138.2	128.6[f]	
		159.0[b]	158.7[b]	158.6[b]	158.3[b]							
2b	228	162.6	127.3	138.0	127.3	154.5	135.4	130.0	46.1	135.5	127.4[f]	
		157.7[b]	156.5[b]	155.8[b]	154.8[b]		128.1	128.9	19.4[c]	19.3[c]	19.2[c]	18.9[c]
	330	164.4	128.6	139.8	128.4	156.6	134.2	130.6	48.5	138.0	128.6[f]	
		158.9[b]	157.9[b]	157.9[b]	157.4[b]				21.1[c]	21.0[c]	20.9[c]	20.6[c]
3b	228	162.8	124.0	138.2	124.0	155.4	135.4	129.8	46.4	135.6	128.0[f]	
		157.4[b]	157.3[b]	156.5[b]	156.3[b]		128.6	129.6	16.8[c]	16.7[c]	16.4[c]	16.3[c]
	328	164.5	125.8	139.9	125.5	157.5	134.1	130.7	48.6	138.1	128.5[f]	
		158.9[b]	158.8[b]	158.4[b]	158.3[b]				18.2[c]	18.1[c]	18.0[c]	17.9[c]
4b	208	162.4	124.3	138.6	124.1	155.5	135.6	129.4	45.4	135.5	128.5[f]	
		164.6[b]	164.6[b]	164.5[b]	163.0[b]		128.5	129.3				
	330	164.1	126.6	140.6	126.1	157.6	134.1	131.0	48.1	138.2	130.3[f]	
		166.3[b]	166.2[b]	166.2[b]	164.7[b]							
5b	223	162.8	124.4	138.8	124.3	156.1	135.9	129.9	45.9[g]	136.0	129.2[f]	
		163.9[b]	163.9[b]	163.7[b]	162.0[b]		128.7	129.3	15.5[c]	15.2[c]	15.1[c]	15.0[c]
	328	164.4	126.5	140.7	126.2	158.9	134.0	131.0	48.3[h]	138.3	130.7[f]	
		165.1[b]	165.0[b]	164.7[b]	163.3[b]				16.0[c]	16.0[c]	15.6[c]	15.5[c]

[a] At 75.56 MHz, in [D_6]acetone; δ in ppm with respect to TMS. [b] C^6 carbon atoms of the *N,N* ligand. [c] Methyl signals of the *N,N* ligand. [d] CH_2 signals of the ethyl group at δ = 21.9, 21.9, 21.6 and 21.4 ppm. [e] CH_2 signals of the ethyl group at δ = 23.8, 23.7, 23.6 and 23.5 ppm. [f] CCl signal. [g] CH_2 signals of the ethyl group at δ = 21.0, 21.9, 21.7 and 21.5 ppm. [h] CH_2 signals of the ethyl group at δ = 23.6, 23.5, 23.4 and 23.2 ppm.

anions and the oxygen atom of the acetone with the hydrogen atoms of the dps ligands [at a distance of 2.443(5) Å]. The geometry about the ruthenium(II) ion is distorted octahedral (Figure 7), with the coordination polyhedron defined by five nitrogen atoms and one sulfur atom: two *N,N*-chelate dps ligands are *cis* to each other while the molecule of 2-pyridyl 2-pyridylmethyl sulfide is bidentate through S(3) and N(5). The distortion of the geometry is mainly caused by the sulfur atom, with a significantly longer Ru−S(3) distance [2.370(1) Å] than the five similar Ru−N bonds [mean 2.104(5) Å, with a slightly shorter bond to N(2) due to the sulfur *trans* effect]. Despite the different size of the chelating rings (6 atoms for dps and 5 for the 2-pyridylmethyl sulfide), the bite angles of the three bidentate ligands are almost equal and N(5)−Ru−S(3) is only slightly narrower than the other two equal chelating angles corresponding to dps molecules [81.39(9)° vs. 89.3(1)°]. The same Ru^{II} coordination has already been observed in our previous work[19] for the $[Ru(N,N'\text{-dps})_2(N,S\text{-dps})]^{2+}$ cation, where the distortion is more important due to the significantly shorter N···S bite of one dps, which closes the corresponding chelating angle up to 67.8(2)°. The larger steric hindrance for the bigger bite and bulk of 2-pyridyl 2-pyridylmethyl sulfide with respect to the *N,S*-dps chelating ligand might be related to the significant elongation of the Ru−N bonds in the corresponding complex [mean value 2.104(5) vs. 2.078(5) Å, respectively]. Moreover, the elongation of the distance to the N atom in the *trans* position causes a contraction the Ru−S(3) bond [2.370(1) vs. 2.424(2) Å, respectively]. However, the Ru−N bonds are still significantly longer than the analogous distances in the known Ru(bipy) complexes due to the reduction in back bonding when dps replaces bipy ligands, as evidenced in the previous work. The dps ligand adopts a twisted *N,N*-inside "butterfly-like" arrangement and the resulting six-membered chelate rings show the usual boat conformation, as evidenced by the

puckering analysis[22] on the Ru/N1/C1/S1/C6/N2 [Ru/N3/C16/S2/C11/N4] ring: θ = 90.8(2)° [92.4(2)]°, φ = 0.7(7)° [4.6(2)]°, QT = 0.847(5) [0.920(2)] Å and Δ_S(Ru) = 0.008(2) [0.045(2)]. The C and N atoms lie on a plane from which the Ru and S atoms deviate by 0.7516(3) [0.8584(3)] Å and 0.718(1) [0.741(1)] Å on the same side, respectively. The two chiral atoms [Ru and S(3)] in the cation might generate two possible couples of enantiomers of the complex and, due to the presence of a crystallographic centre of symmetry, the crystal packing is a racemic mixture corresponding to the couple $\Delta S/\Lambda R$ (one arbitrary enantiomer of which is represented in Figure 7).

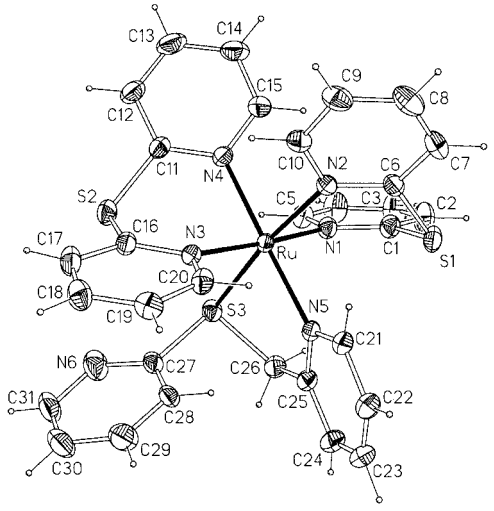

Figure 7. View of the cation **1c**·C_3H_6O showing the labelling scheme; anions and co-crystallized acetone moieties have been omitted for clarity; thermal ellipsoids are drawn at 50% probability while the size of the hydrogen atoms is arbitrary

Discussion

Our previous studies[19] on the dynamic behaviour of [Ru(*N*,*N*-dprs)$_2$(*N*,*S*-phpys)][PF_6]$_2$ and [Ru(*N*,*N*-dps)$_2$(*N*,*S*-phpys)][PF_6]$_2$ (phpys = phenyl pyridyl sulfide), containing a four-membered RuSCN(*Ru*−*N*) ring, showed that, in the range 180−240 K, a restricted rotation of the pendant phenyl ring was operative, affecting only the phenyl proton signals. Above 240 K extensive internal arrangements were invoked to explain the changes in the aromatic region of the ^{1}H NMR spectra at higher temperature.

The ^{1}H NMR spectra of the complexes containing a four-membered RuSCN(*Ru*−*N*) ring — [Ru(*N*,*N*-diimine)(*N*,*S*-pySCH_2R)][PF_6]$_2$ or [Ru(*N*,*N*-diimine)$_2$(*N*,*S*-prSCH_2R)][PF_6]$_2$ [20] — at the lowest temperature reached (190 K) clearly show the presence of two slowly exchanging invertomers, and restricted rotation is not observed. It is likely that restricted rotation of the phenyl group occurs below 190 K but experimental difficulties ruled out the possibility of confirming this proposal. Furthermore, for these complexes, which contain a chiral ruthenium atom (configurations Δ and Λ) and a chiral sulfur atom [configurations (*S*) and (*R*)] the possibility of racemisation ($\Delta \rightleftarrows \Lambda$) was discarded and only the sulfur inversion [(*R*) $\rightleftarrows$ (*S*)] occurred.

In this work owing to the *N*,*S* chelation of the thioethers **a** and **b** and the consequent formation of a five-membered metallacycle, two invertomers, as the enantiomeric couples $\Delta R/\Lambda S$ and $\Delta S/\Lambda R$, are expected and, consequently, two AB systems for the methylene protons in the ^{1}H NMR spectra. However, the spectra only show a single AB system. This can indicate the presence of: (i) only one invertomer, (ii) two invertomers that give superimposed signals, or (iii) two rapidly exchanging invertomers at low temperatures. The presence of only one invertomer or two invertomers that give superimposed signals, should eliminate the possibility of a rotation process exchanging the *ortho*- as well as the *meta*-phenyl protons, whereas the NOESY experiments indicate the exchange of the phenyl protons.

It is important to note at this point that the splitting patterns of the methylene protons (single AB system) and phenyl protons (coupling constants between **M** and **N** as well as **O** and **P)** rule out the possibility of a slow sulfur inversion at low temperatures, while the splitting patterns of the methylene protons at higher temperatures (single AB system) also rule out the possibility of racemisation ($\Delta \rightleftarrows \Lambda$) which should average the environments of the methylene protons. In other words, due to the very fast sulfur inversion even at low temperatures, averaged methylene proton signals as well as averaged phenyl proton signals of the two invertomers were observed, whereas due to the restricted phenyl rotation the two *ortho*- (and *meta*-) phenyl protons are anisochronous. The fast rotation of the phenyl ring at high temperatures makes the averaged environments of the two *ortho*- (and *meta*-) protons equivalent, whereas the methylene protons are practically unaffected.

On the other hand, from literature precedents it is unlikely that the two invertomers have similar resonances. In particular, the methylene proton signals are very sensitive to the sulfur configurations and four doublets are observed in the methylene region when two slowly exchanging invertomers are present.[20,23,24] Furthermore, the H^3 pyridine proton of the *N*,*S*-chelate ligand and the other pyridine and pyrimidine protons gave well-separated signals for the two invertomers at low temperature,[20] whereas for the present compounds only a single signal is present. Thus, two rapidly exchanging invertomers are present. In order to firmly establish this point and other structural features we attempted several crystallizations of the present compounds. None of the complexes containing ligands **a** or **b** gave crystals suitable for X-ray crystallography; however, the reaction of 2-pyridyl 2-pyridylmethyl sulfide (**c**) and [$RuCl_2$(dps)$_2$] in the presence of NH_4PF_6 gave [Ru(*N*,*N*-dps)$_2$(*N*,*S*-**c**)][PF_6]$_2$ (**1c**) which easily formed crystals. The X-ray analysis revealed the enantiomeric couple $\Delta S/\Lambda R$. Moreover, the ^{1}H NMR spectra of this complex are compatible with the presence of two rapidly exchanging invertomers: a single AB system is observed for the methylene protons at low temperatures (Table 1).

For the complexes [*cis*-Ru(*N*,*N*-diimine)(*N*,*S*-pySCH$_2$R)][PF$_6$]$_2$ and [*cis*-Ru(*N*,*N*-diimine)$_2$(*N*,*S*-prSCH$_2$R)][PF$_6$]$_2$ [20] the access to the transition state of sulfur inversion is difficult due to the four-membered chelate ring. However, the relatively high-energy ground state, due to the simultaneous presence of the congested Ru(diimine)$_2$ fragment and the sterically demanding four-membered *N*,*S*-chelate ring, explains the low energy-barrier of the process. In the present complexes the steric demand of the Ru(diimine)$_2$ fragments is similar, whereas the increase of the chelate ring-size decreases the transition-state energy of the inversion, which consequently is fast. Therefore, the only fluxional process observed which exchanges the *ortho*- and *meta*-protons (whereas other protons are practically unchanged) is a phenyl rotation. The possible mechanisms that need to be considered are: (i) a dissociative mechanism with formation of five-coordinate species in which exchange of the two halves of the phenyl ring is operative, (ii) an associative mechanism involving solvent, anion or free ligand with formation of a seven-coordinate species in which restricted rotation of phenyl ring occurs, or (iii) phenyl rotation in the octahedral complexes without any bond rupture. The dissociative mechanism can be discarded on the basis of the following findings: (i) the NMR spectra are temperature-reversible and concentration-independent, (ii) the exchange rates are similar in acetone and acetonitrile, (iii) the steric hindrance to phenyl rotation can be very much diminished by dissociation of the Ru−S or Ru−N bond; and (iv) in the presence of a Ru−S bond dissociation the sulfur inversion and phenyl rotation would occur at the same rate. On the contrary, at low temperatures, sulfur inversion is fast whereas phenyl rotation is slow. An associative mechanism involving solvent, anion or free ligand is also unlikely. In fact, when the free ligand is added, separate signals are observed and the exchange rates are not affected. Addition of chloride or hexafluorophosphate anion does not affect the rate of the process. Therefore, the only mechanism consistent with all the experimental results appears to be the phenyl rotation in the octahedral complexes. This phenyl rotation occurs at higher rates in the complexes containing Ru(dprs)$_2$ or Ru(5edprs)$_2$ fragments than in those containing Ru(dps)$_2$, Ru(4mdps)$_2$ or Ru(5mdps)$_2$ fragments, the differences in the averaged $\Delta G^{\#}_{298}$ values being 4 kJ·mol^{-1} (Table 3); the substitution of dps with 4mdps or 5mdps leaves the magnitude of $\Delta G^{\#}_{298}$ practically unchanged. Similarly, substitution of dprs with 5edprs or **a** with **b** does not affect the values of $\Delta G^{\#}_{298}$. On this basis we suggest that the contribution of electronic effects to the restricted phenyl rotation is negligible while the parameters observed are correlated to the hindrance produced by the two ligands *cis* to the rotating group. Crystallographic data of [Ru(*N*,*N*-dps)$_2$(*N*,*S*-**c**)][PF$_6$]$_2$ and similar complexes[15,18,19] indicate that *N*,*N* chelation is favoured by the combination of the boat conformation for the six-membered metallacycle and a twisted *N*,*N*-inside conformation of dps which corresponds to the best pyridine dihedral angle for chelation to the metal atom. We have no crystallographic data of dprs complexes containing **a** or **b** or other *N*,*S* ligands; however, it is very likely that the conformation of the *N*,*N* chelate dprs is similar. Since the pyridine or pyrimidine rings are inclined the hindrance to rotation is mainly determined by the size of the N atom and, to a lesser extent, by the CH[6] group. In other words, the inclined pyrimidine ring of dprs is somewhat "bulkier" than the inclined pyridine ring of dps, producing enhanced hindrance to the phenyl rotation.

Conclusion

The reactions of a series of thioethers bearing CH$_2$Py groups has allowed us to extend the chemistry of polypyridylruthenium(II) compounds containing *N*,*S*-coordinated ligands with a five-membered chelate ring. The NMR experiments clearly show that the phenyl rotation in the octahedral complexes is the fluxional process that produces the exchange of the *ortho*- and *meta*-phenyl protons. The steric hindrance of the ruthenium substrates appears to play a determinant role for the phenyl rotation which, in the complexes containing dps ligands or methyl derivatives, occurs at lower rates than in those containing dprs or 5edprs; the difference in the averaged $\Delta G^{\#}$ values being 4 kJ·mol^{-1}. The ring size of the *N*,*S*-coordinated thioether ligand plays a determinant role for the sulfur inversion. When the inverting sulfur atom is present in a five-membered *N*,*S*-chelated ring, the process is fast even at low temperatures, whereas in a four-membered ring[20] it is much slower. Further experiments are in progress with the aim of studying the effect of the nature of congested Ru(*N*,*N*-diimine)$_2$ cores and sterically demanding thioethers on the energy barrier of the dynamic processes.

Experimental Section

General Remarks: Di-2-pyridyl sulfide,[25] di-2-pyrimidyl sulfide,[19] 2-pyridylmethyl *p*-tolyl sulfide,[26] *p*-chlorophenyl 2-pyridylmethyl sulfide,[26] 2-pyridyl 2-pyridylmethyl sulfide,[26] [RuCl$_2$(dps)$_2$]·2H$_2$O[15] and [RuCl$_2$(dprs)$_2$]·2H$_2$O[19] were prepared by published methods. Other reagents and solvents were used as received. Conductivity measurements were done with a Radiometer CDM 3 conductivity meter. Infrared spectra were recorded with an FT-IR 1720X spectrophotometer with samples as Nujol mulls placed between KBr plates and the ^{1}H and ^{13}C NMR spectra with a Bruker AMX 300 spectrometer. The following Bruker programs were used: zg, homodecnew, zgpg, jmod, cosy, noesy.pt, invb. Simulations of static and dynamic spectra were performed with the G NMR program. Selected ^{1}H NMR spectroscopic data for the complexes are given in Tables 1 and 2, activation energy data are given in Table 3 and ^{13}C NMR spectroscopic data are given in Table 4.

2,2′-Bis(5-ethylpyrimidyl) Sulfide (5edprs): 2-Chloro-5-ethylpyrimidine (4.85 g, 34.0 mmol) was dissolved in *N*,*N*-dimethylformamide (30 mL), under N$_2$. Na$_2$S (1.37 g, 17.5 mmol) was added. The resulting mixture was heated to reflux with stirring for 4 h. The initial pale-yellow solution gradually turned green, then deep yellow. The solvent was distilled off under reduced pressure and the residue extracted with CH$_2$Cl$_2$. Evaporation of the solvent gave a pale-yellow solid, which was crystallized from CH$_2$Cl$_2$ (30 mL) by care-

ful addition of heptane, washed with pentane and dried in vacuo. Yield 1.26 g (30%). Selected IR data (KBr): $\tilde{\nu}$ = 1607 ms, 1574 s, 1538 vs, 1267 s, 1230 vs, 1142 vs, 1068 s, 938 vs, 820 vs, 790 s, 767 vs, 653 vs, 646 vs 638 vs, 499 vs cm^{-1}. ^1H NMR ([D$_6$]acetone, 298 K): δ = 1.25 (t, $^3J_{H,H}$ = 7.6 Hz, 6 H, CH_3), 2.67 (q, 4 H, CH_2), 8.56 (s, 4 H, H^3 and H^6) ppm. $^{13}C\{^1H\}$ NMR ([D$_6$]acetone, 298 K): δ = 15.05 (CH_3), 23.45 (CH_2), 158.25 (C^3 and C^6) ppm. $C_{12}H_{14}N_4S$ (246.33): calcd. C 58.51, H 5.73, N 22.74, S 13.01; found C 58.40, H 5.80, N 22.60, S 13.00.

2,2′-Bis(4-methylpyridyl) Sulfide (4mdps):[21] 2-Bromo-4-methylpyridine (9.70 g, 56.4 mmol) was dissolved in *N*,*N*-dimethylformamide (30 mL) under N_2. Na_2S (2.28 g, 29.2 mmol) was added. The resulting mixture was heated to reflux with stirring for 6 h. The initial pale-yellow solution gradually turned green, then yellow. Distillation under reduced pressure gave the solvent at 30−50 °C and the compound as a yellow oil at 150 °C. The oil was kept at −24 °C until it solidified. Selected IR data (KBr): $\tilde{\nu}$ = 1625 s, 1590 vs, 1556 s, 1539 s, 1282 ms, 1233 s, 1221 s, 1119 vs, 1079 vs, 986 s, 869 ms, 849 vs, 823 vs, 700 vs, 539 s, 517 s cm^{-1}. ^1H NMR ([D$_6$]acetone, 298 K): δ = 2.30 (s, 6 H, CH_3), 7.09 (dd, $J_{6,5}$ = 5.0 Hz, $J_{5,3}$ = 1.3 Hz, 2 H, H^5), 7.31 (d, 2 H, H^3), 8.33 (d, 2 H, H^6) ppm. $^{13}C\{^1H\}$ NMR ([D$_6$]acetone, 298 K): δ = 20.60 (CH_3), 123.50 (C^5), 126.70 (C^3), 150.30 (C^6) ppm.

2,2′-Bis(5-methylpyridyl) Sulfide (5mdps):[21] The compound was obtained in the same way as above starting from 2-bromo-5-methylpyridine (9.70 g, 56.4 mmol) and Na_2S (1.37 g, 17.5 mmol). Selected IR data (KBr): $\tilde{\nu}$ = 1667 vs, 1586 vs, 1557 vs, 1504 s, 1221 vs, 1102 vs, 1084 s, 1025 vs, 828 vs, 724 s cm^{-1}. ^1H NMR ([D$_6$]acetone, 298 K): δ = 2.30 (s, 6 H, CH_3), 7.32 (d, $J_{4,3}$ = 8.1 Hz, 2 H, H^3), 7.54 (dd, $J_{6,4}$ = 2.2 Hz, 2 H, H^4), 8.33 (d, 2 H, H^6) ppm. $^{13}C\{^1H\}$ NMR ([D$_6$]acetone, 298 K): δ = 17.80 (CH_3), 125.90 (C^3), 138.40 (C^4), 151.05 (C^6) ppm.

[RuCl$_2$(*N*,*N*-4mdps)$_2$] (2): $RuCl_3 \cdot 3H_2O$ (1 g, 3.8 mmol), LiCl (1 g, 23.6 mmol) and 4mdps (1.65 g, 7.63 mmol) were refluxed in DMF (30 mL) under N_2 for 4 h. After cooling to room temperature and addition of acetone (30 mL), the mixture was allowed to stand at 4 °C overnight giving a dark-red solid which was filtered and washed with acetone. The compound was dried over P_4O_{10} in vacuo. Yield 0.92 g (40%). Selected IR data (KBr): $\tilde{\nu}$ = 1650 br, 1599 vs, 1282 s, 1140 s, 1082 s, 820 vs, 720 s cm^{-1}. ^1H NMR ($CDCl_3$, 298 K): δ = 2.23 (s, 6 H, CH_3), 2.34 (s, 6 H, CH_3), 6.62 (dd, $J_{6,5}$ = 6.0 Hz, $J_{5,3}$ = 1.9 Hz, 2 H, H^5), 7.13 (dd, $J_{6,5}$ = 6.0 Hz, $J_{5,3}$ = 1.9 Hz, H^5), 2 H, 7.14 (d, 2 H, H^3),7.31 (d, 2 H, H^3),8.30 (d, 2 H, H^6), 10.04 (d, 2 H, H^6) ppm. $C_{24}H_{24}Cl_2N_4RuS_2$ (604.58): calcd. C 47.68, H 4.00, N 9.27, S 10.61; found C 47.80, H 4.00, N 9.35, S 10.60.

[RuCl$_2$(*N*,*N*-5mdps)$_2$] (3): $RuCl_3 \cdot 3H_2O$ (1 g, 3.8 mmol), LiCl (1 g, 23.6 mmol) and 5mdps (1.65 g, 7.63 mmol) were refluxed in DMF (20 mL) under N_2 for 5 h. The solution was cooled to room temperature and 40 mL of acetone added. The mixture was allowed to stand at −24 °C overnight. An orange-red solid had formed which was filtered, washed with acetone/diethyl ether mixtures [2:1 (21 mL), 1:1 (30 mL) and 1:3 (40 mL)] and dried over P_4O_{10} in vacuo. Yield 1.03 g (45%). Selected IR data (KBr): $\tilde{\nu}$ = 1630 br, 1589 s, 1284 s, 1234 s, 1136 vs, 1101 vs, 822 vs, 722 s, 532 s cm^{-1}. ^1H NMR ([D$_6$]acetone, 298 K): δ = 2.01 (s, 6 H, CH_3), 2.41 (s, 6 H, CH_3), 7.33 (dd, $J_{4,3}$ = 7.9 Hz, $J_{6,3}$ = 0.8 Hz, 2 H, H^3), 7.38 (dd, $J_{4,3}$ = 7.9 Hz, $J_{6,4}$ = 2.5 Hz, 2 H, H^4), 7.53 (dd, $J_{4,3}$ = 7.9 Hz, $J_{6,3}$ = 0.8 Hz, 2 H, H^3), 7.62 (dd, $J_{4,3}$ = 7.9 Hz, $J_{6,4}$ = 2.5 Hz, 2 H, H^4), 8.30 (dd, 2 H, H^6), 10.04 (dd, 2 H, H^6) ppm. $C_{24}H_{24}Cl_2N_4RuS_2$ (604.58): calcd. C 47.68, H 4.00, N 9.27, S 10.61; found C 47.60, H 4.10, N 9.30, S 10.70.

[Ru(*N*,*N*-5edprs)$_2$Cl$_2$] (4): This red compound was obtained in the same way as above, starting from $RuCl_3 \cdot 3H_2O$ (1 g, 3.8 mmol), LiCl (1 g, 23.6 mmol) and 5etdprs (1.94 g, 7.63 mmol). Yield 0.88 g (35%). Selected IR data (KBr): $\tilde{\nu}$ = 1675 vs, 1540 vs, 1220 s, 1182 vs, 1136 vs, 1058 vs, 910 vs, 822 vs, 752vs, 740 vs 720 s, 662 s cm^{-1}. ^1H NMR ([D$_6$]acetone, 298 K): δ = 1.02 (t, $^3J_{H,H}$ = 7.6 Hz, 6 H, CH_3), 1.34 (t, $^3J_{H,H}$ = 7.6 Hz, 6 H, CH_3), 2.48 (q, 4 H, CH_2), 2.78 (q, 4 H, CH_2), 8.34 (dd, $J_{4,3}$ = 7.9 Hz, $J_{6,4}$ = 2.6 Hz, 2 H, H^4), 8.49 (dd, $J_{6,4}$ = 2.6 Hz, 2 H, H^6), 8.59 (d, $J_{6,4}$ = 2.8 Hz, 2 H, H^4), 10.01 (d, $J_{6,4}$ = 2.8 Hz, 2 H, H^6). $C_{24}H_{28}Cl_2N_8RuS_2$ (664.64): calcd. C 43.37, H 4.24, N 16.86, S 9.65; found C 43.50, H 4.30, N 17.00, S 9.70.

[Ru(*N*,*N*-dps)$_2$(*N*,*S*-a)][PF$_6$]$_2$ (1a): $[RuCl_2(dps)_2] \cdot 2H_2O$ (0.195 g, 0.33 mmol) and 2-pyridylmethyl *p*-tolyl sulfide (0.286 g, 1.33 mmol) were refluxed in 50 mL of ethanol/water (3:2) under N_2 for 4 h. After filtration of the solution into 80 mL of water containing NH_4PF_6 (0.49 g, 3 mmol), a yellow precipitate was obtained, filtered, washed with cold water (30 mL) and dried overnight. The solid was then dissolved in acetone (15 mL), precipitated with diethyl ether (100 mL), washed with diethyl ether (70 mL) and dried over P_4O_{10} under vacuum. Yield 0.165 g (50%). Selected IR data (KBr): $\tilde{\nu}$ = 1589 vs, 1561 ms, 1284 s, 1165 s, 878 vs, 843 br, 770 vs, 741 ms, 727 s, 558 vs cm^{-1}. $C_{33}H_{29}F_{12}N_5P_2RuS_3$ (982.81): calcd. C 40.33, H 2.97, N 7.12; found C 40.15, H 3.05, N 7.10. Conductivity: Λ_M (MeCN, 2 × 10^{-4} mol·dm^{-3}, 25 °C) = 316 S·cm^2·mol^{-1}.

[Ru(*N*,*N*-5mdps)$_2$(*N*,*S*-a)][PF$_6$]$_2$ (3a): The compound was obtained in the same way as **1a**, starting from $[RuCl_2(5mdps)_2]$ (0.201 g, 0.33 mmol) and 2-pyridylmethyl *p*-tolyl sulfide (0.286 g, 1.33 mmol). Yield 0.220 g (64%). Selected IR data (KBr): $\tilde{\nu}$ = 1667 s, 1597 s, 1565 ms, 1494 vs, 1283 vs, 1240 vs, 1120 vs, 1106 s, 877 vs, 840 br, 775 vs, 740 s, 725 ms, 557 vs, 530 vs cm^{-1}. $C_{37}H_{37}F_{12}N_5P_2RuS_3$ (1038.9): calcd. C 42.78, H 3.59, N 6.74; found C 42.90, H 3.60, N 6.80. Conductivity: Λ_M (MeCN, 2 × 10^{-4} mol·dm^{-3}, 25 °C) = 328 S·cm^2·mol^{-1}.

[Ru(*N*,*N*-dprs)$_2$(*N*,*S*-a)][PF$_6$]$_2$ (4a): $[RuCl_2(dprs)_2] \cdot 2H_2O$ (0.196 g, 0.33 mmol) and 2-pyridylmethyl *p*-tolyl sulfide (0.286 g, 1.33 mmol) were heated to reflux in 50 mL of ethanol/water (3:2). After 3 h, the solution was filtered and 50 mL of water containing NH_4PF_6 (0.65 g, 4 mmol) was added. The mixture was heated for 2 h. The solution obtained was allowed to stand until a brown precipitate was formed, which was filtered, washed with water, and dried overnight. The solid was then dissolved in acetone (10 mL) and added to the top of a chromatography column (diameter 2 cm) packed with aluminium oxide (50 g; Aldrich, neutral, 150 mesh, deactivated with water 0.15 g). Elution with CH_2Cl_2/acetone (3:2) gave a yellow-orange band which was collected, concentrated (10 mL) and precipitated with diethyl ether (50 mL). The solid obtained was washed with diethyl ether (50 mL) and dried over P_4O_{10} under vacuum. Yield 0.130 g (40%). Selected IR data (KBr): $\tilde{\nu}$ = 1604 ms, 1561 s, 1547 s, 1164 s, 1084 ms, 1014 ms, 876vs, 842 br, 762 vs, 751 ms, 722 ms, 649 ms, 597 ms, 558 vs cm^{-1}. $C_{29}H_{25}F_{12}N_9P_2RuS_3$ (986.76): calcd. C 35.30, H 2.55, N 12.78; found C 35.20, H 2.60, N 12.80. Conductivity: Λ_M (MeCN, 2 × 10^{-4} mol·dm^{-3}, 25 °C) = 305 S·cm^2·mol^{-1}.

[Ru(*N*,*N*-5edprs)$_2$(*N*,*S*-a)][PF$_6$]$_2$ (5a): This compound was prepared by refluxing a mixture of $[RuCl_2(5edprs)_2]$ (0.332 g, 0.50 mmol) and 2-pyridylmethyl *p*-tolyl sulfide (0.646 g, 3.0 mmol) in 50 mL of ethanol/water (3:2) under N_2 for 5 h. After filtration of the solution into 80 mL of water containing NH_4PF_6 (0.49 g, 3 mmol) an orange precipitate was obtained, which was filtered and dried overnight. The crude product was dissolved in acetone (10 mL) and

added to the top of a chromatography column (diameter 2 cm) packed with aluminium oxide (50 g; Aldrich, neutral, 150 mesh, deactivated with water 0.15 g). Elution with CH_2Cl_2/acetone (3:2) gave a yellow-orange band which was collected, concentrated (10 mL) and the product precipitated with diethyl ether (50 mL). The solid obtained was washed with diethyl ether (50 mL) and dried over P_4O_{10} under vacuum. Yield 0.220 g (40%). Selected IR data (KBr): $\tilde{\nu}$ = 1667 s, 1581 s, 1544 vs, 1234 s, 1187s, 1142 s, 1060 s, 880 vs, 843 br, 755 vs, 740 vs, 727 s, 663 s, 557 cm^{-1}. $C_{37}H_{41}F_{12}N_9P_2RuS_3$ (1099.0): calcd. C 40.44, H 3.76, N 11.47; found C 44.50, H 3.80, N 11.40. Conductivity: Λ_M (MeCN, 2×10^{-4} mol·dm^{-3}, 25 °C) = 310 S·cm^2·mol^{-1}.

[Ru(*N*,*N*-dps)$_2$(*N*,*S*-b)][PF$_6$]$_2$ (1b): This yellow compound was prepared in the same way as **1a**, starting from [$RuCl_2$(dps)$_2$]·$2H_2O$ (0.195 g, 0.33 mmol) and *p*-chlorophenyl 2-pyridylmethyl sulfide (0.313 g, 1.33 mmol). Yield 0.160 g (48%). Selected IR data (KBr): $\tilde{\nu}$ = 1589 s, 1284 s, 1164 s, 1094 vs, 1011 s, 879 vs, 847 br, 770 vs, 744 ms, 726 ms, 558 vs, 508 ms cm^{-1}. $C_{32}H_{26}ClF_{12}N_5P_2RuS_3$ (1003.2): calcd. C 38.31, H 2.61, N 6.98; found C 38.10, H 2.65, N 7.00. Conductivity: Λ_M (MeCN, 2×10^{-4} mol·dm^{-3}, 25 °C) = 307 S·cm^2·mol^{-1}.

[Ru(*N*,*N*-4mdps)$_2$(*N*,*S*-b)][PF$_6$]$_2$ (2b): This yellow compound was prepared in a similar fashion to **1a**, starting from [$RuCl_2$(4mdps)$_2$] (0.201 g, 0.33 mmol) and *p*-chlorophenyl 2-pyridylmethyl sulfide (0.313 g, 1.33 mmol). Yield 0.180 g (51%). Selected IR data (KBr): $\tilde{\nu}$ = 1674 s, 1605 vs, 1288 s, 1093 vs, 1011 vs, 878 vs, 843 br, 776 vs, 740 vs, 720 s, 557 vs, 508 s, 499 s cm^{-1}. $C_{32}H_{26}ClF_{12}N_5P_2RuS_3$ (1059.3): calcd. C 40.82, H 3.24, N 6.61; found C 40.90, H 3.30, N 6.60. Conductivity: Λ_M (MeCN, 2×10^{-4} mol·dm^{-3}, 25 °C) = 318 S·cm^2·mol^{-1}.

[Ru(*N*,*N*-5mdps)$_2$(*N*,*S*-b)][PF$_6$]$_2$ (3b): This yellow compound was prepared in the same way as **1a**, starting from [$RuCl_2$(5mdps)$_2$] (0.201 g, 0.33 mmol) and *p*-chlorophenyl 2-pyridylmethyl sulfide (0.313 g, 1.33 mmol). Yield 0.200 g (56%). Selected IR data (KBr): $\tilde{\nu}$ = 1678 vs, 1605 s, 1598 s, 1568 s, 1283 s, 1241 s, 1119 vs, 1092 vs, 1009 vs, 876 vs, 836 br, 764 vs, 741 s, 725 ms, 558 vs, 530 s, 512 s cm^{-1}. $C_{36}H_{34}ClF_{12}N_5P_2RuS_3$ (1059.3): calcd. C 40.82, H 3.24, N 6.61, S 9.08; found C 40.80, H 3.30, N 6.70, S 9.10. Conductivity: Λ_M (MeCN, 2×10^{-4} mol·dm^{-3}, 25 °C) = 307 S·cm^2·mol^{-1}.

[Ru(*N*,*N*-dprs)$_2$(*N*,*S*-b)][PF$_6$]$_2$ (4b): This orange compound was obtained in the same way as **1a**, starting from [$RuCl_2$(dprs)$_2$]·$2H_2O$ (0.196 g, 0.33 mmol) and *p*-chlorophenyl 2-pyridylmethyl sulfide (0.313 g, 1.33 mmol). Yield 0.151 g (45%). Selected IR data (KBr): $\tilde{\nu}$ = 1579 vs, 1575 vs, 1548 vs, 1167 vs, 1096 s, 1011 s, 874 vs, 846 br, 767 s, 753 vs, 742 ms, 558 vs, 509 ms cm^{-1}. $C_{28}H_{22}ClF_{12}N_9P_2RuS_3$ (1007.2): calcd. C 33.37, H 2.20, N 12.52; found C 33.30, H 2.30, N 12.50. Conductivity: Λ_M (MeCN, 2×10^{-4} mol·dm^{-3}, 25 °C) = 309 S·cm^2·mol^{-1}.

[Ru(*N*,*N*-5edprs)$_2$(*N*,*S*-b)][PF$_6$]$_2$ (5b): This orange compound was prepared and purified in the same way as **5a**, starting from [$RuCl_2$(5edprs)$_2$] (0.332 g, 0.50 mmol) and *p*-chlorophenyl 2-pyridylmethyl sulfide (0.707 g, 3.0 mmol). Yield 0.252 g (45%). Selected IR data (KBr): $\tilde{\nu}$ = 1667 vs, 1580 s, 1548 vs, 1243 s, 1143 s, 1095 s, 1061 s, 1011 s, 880 vs, 846 br, 762 s, 757 s, 558 vs cm^{-1}. $C_{36}H_{38}ClF_{12}N_9P_2RuS_3$ (1119.4): calcd. C 38.63, H 3.42, N 11.26, S 8.59; found C 38.60, H 3.55, N 11.20, S 8.60. Conductivity: Λ_M (MeCN, 2×10^{-4} mol·dm^{-3}, 25 °C) = 284 S·cm^2·mol^{-1}.

[Ru(*N*,*N*-dps)$_2$(*N*,*S*-c)][PF$_6$]$_2$ (1c): This yellow compound was obtained in the same way as **4a**, starting from [$RuCl_2$(dps)$_2$]·$2H_2O$ (0.195 g, 0.33 mmol) and 2′-pyridyl 2-pyridylmethyl sulfide (0.178 g, 0.882 mmol) Yield 0.226 g (70%). Selected IR data (KBr): $\tilde{\nu}$ = 1610 ms, 1588 s, 1571 s, 1561 ms, 1284 s, 1165 s, 1130 ms, 1089 ms, 878 s, 845 br, 769 vs, 741 s, 727 ms, 558 vs, 528 ms cm^{-1}. $^{13}C\{^1H\}$ NMR ([D_6]acetone, 298 K): δ = 45.9 (CH_2), 123.6 (C^5_c), 124.0, 125.4, 126.0, 126.7 (4 C^5_{dps}), 127.2 (C^5_c), 127.5 (C^3_c), 128.7, 128.8, 129.6, 130.2 (4 C^3_{dps}), 130.4 (C^3_c), 138.4 (C^4_c), 138.6, 139.3, 139.7, 140.0 (4 C^4_{dps}), 140.4 (C^4_c), 150.1 (C^6_c), 153.8 (C^2_c), 156.6 (C^2_{dps}), 157.1 (C^6_c), 157.1 (C^6_{dps}), 157.5 (C^2_{dps}), 157.9 (C^6_{dps}), 158.1 (C^2_{dps}), 158.4, 158.7 (2 C^6_{dps}), 159.2 (C^2_{dps}), 165.0 (C^2_c). $C_{31}H_{26}F_{12}N_6P_2RuS_3$ (969.77): calcd. C 38.40, H 2.70, N 8.67, S 9.92; found C 38.35, H 2.80, N 8.60, S 9.90. Conductivity: Λ_M (MeCN, 2×10^{-4} mol·dm^{-3}, 25 °C) = 327 S·cm^2·mol^{-1}.

Single-Crystal X-ray Diffraction Study of 1c: Suitable crystals of complex **1c** were obtained by slow evaporation of solvent from a diethyl ether/acetone (1:1) solution. Diffraction data were collected with a Siemens P4 automatic four-circle diffractometer. Lattice parameters were obtained from least-squares refinement of the setting angles of 42 reflections within the 2θ range 6−30°. A summary of the crystallographic data and the structure refinement is reported in Table 5. Monitoring of three standard reflection measurements evidenced no crystal deterioration. The reflection intensities were evaluated by a learnt-profile procedure[27] among 2θ shells and then corrected for Lorentz-polarization effects. Absorption correction was applied by fitting a pseudo-ellipsoid to the azimuthal scan data (0−360% range by a 10% step) of 15 high χ reflections.[28] Data collection and reduction were performed with the XSCANS[29] and SHELXTL[30] package. The structure was solved by a combination of standard Direct Methods[31] and Fourier synthesis, and refined by minimising the function $\Sigma w(F_o^2 - F_c^2)^2$ with the full-matrix least-squares technique based on all independent *F*, using SHELXL-97.[32] All non-hydrogen atoms were refined anisotropically. Hydrogen atoms were included in the model refinement with the "riding

Table 5. Crystallographic data for **1c**·C_3H_6O

Empirical formula	$[C_{31}H_{26}N_6S_3Ru][PF_6]_2$·$(CH_3)_2CO$
Formula mass	1027.85
Crystal dimensions	0.37 × 0.27 × 0.20 mm
Crystal colour and form	yellow, irregular
Crystal system	monoclinic
Space group	$P2_1/c$ (no. 14)
Unit cell dimensions	a = 11.760(1) Å
	b = 13.792(1) Å
	c = 25.883(2) Å
	β = 90.051(8)°
V	4197.8(6) Å^3
Z	4
F(000)	2064
$\rho_{calcd.}$	1.626 g/cm^3
μ	0.689 mm^{-1}
λ (graphite-monochromated)	0.71073 Å (Mo-K_α)
2θ range	4.3−50°
Data collected (2θ-ω)	8597
Data independent (refined)	7369 (R_{int} = 0.0240)
Data observed	5938 [$I \geq 2\sigma(I)$]
Variables	532
Completeness to 2θ = 50°	0.995
$R1$[a] (observed/refined data)	0.0462/0.0617
$wR2$[b] (observed/refined data)	0.1110/0.1210
GOF[c] (observed/refined data)	1.040/1.040
Max. diff. peak and hole	0.588/−0.547 e·Å^{-3}
Max. and mean shift/esd	0.002/0.001

[a] $R = (\Sigma||F_o| - |F_c||)/\Sigma|F_o|$. [b] $Rw = \{\Sigma[w(F_o^2 - F_c^2)^2]/[\Sigma w(F_o^2)^2]\}^{1/2}$. [c] GOF= $\{\Sigma[w(F_o^2 - F_c^2)^2/(N_{obs.} - N_{var.})]\}^{1/2}$.

model'' method with the X−H bond geometry and isotropic displacement parameter depending on the parent X atom. The co-crystallized acetone molecules and hexafluorophosphate anions show large atomic thermal ellipsoids due to the expected rotational disorder of their spherical moieties. Any attempt to represent the biggest ellipsoids as adjacent atomic partial occupancies was unsuccessful. The final geometrical calculations and drawings were carried out with the PARST program[33] and the XPW utility of the Siemens package, respectively. Selected bond lengths and bond angles are reported in Table 6 while Figure 7 represents the complex cation with its atomic labelling scheme. CCDC-226905 contains the supplementary crystallographic data for this paper. These data can be obtained free of charge at www.ccdc.cam.ac.uk/conts/retrieving.html [or from the Cambridge Crystallographic Data Centre, 12 Union Road, Cambridge CB2 1EZ, UK; Fax: + 44-1223-336033; E-mail: deposit@ccdc.cam.ac.uk].

Table 6. Selected bond lengths [Å] and angles [°] for **1c**·C_3H_6O

Ru−N(2)	2.096(3)	Ru−N(1)	2.102(3)
Ru−N(4)	2.103(3)	Ru−N(5)	2.108(3)
Ru−N(3)	2.112(3)	Ru−S(3)	2.370(1)
N(1)−C(5)	1.352(6)	N(1)−C(1)	1.354(6)
C(1)−S(1)	1.768(5)	S(1)−C(6)	1.772(5)
C(6)−N(2)	1.350(5)	C(10)−N(2)	1.352(5)
N(3)−C(20)	1.317(5)	N(3)−C(16)	1.362(5)
S(2)−C(16)	1.769(5)	C(11)−S(2)	1.771(5)
C(11)−N(4)	1.340(5)	C(15)−N(4)	1.355(6)
N(5)−C(21)	1.346(5)	N(5)−C(25)	1.358(5)
C(25)−C(26)	1.478(7)	C(26)−S(3)	1.829(5)
C(27)−S(3)	1.822(5)	C(27)−N(6)	1.404(7)
C(31)−N(6)	1.407(8)		
N(2)−Ru−N(1)	89.3(1)	N(2)−Ru−N(4)	86.1(19
N(1)−Ru−N(4)	86.6(1)	N(2)−Ru−N(5)	92.9(1)
N(1)−Ru−N(5)	92.9(1)	N(2)−Ru−N(3)	93.1(1)
N(4)−Ru−N(3)	89.3(1)	N(5)−Ru−N(3)	91.2(1)
N(1)−Ru−S(3)	86.6(1)	N(4)−Ru−S(3)	99.6(1)
N(5)−Ru−S(3)	81.39(9)	N(3)−Ru−S(3)	91.4(1)
C(1)−S(1)−C(6)	103.5(2)	C(16)−S(2)−C(11)	103.5(2)
C(25)−C(26)−S(3)	111.7(3)	C(27)−S(3)−C(26)	97.6(2)

Acknowledgments

This work was supported by the Università of Messina, Italy (PRA, **2001**).

[1] D. C. Black, *Aust. J. Chem.* **1967**, *20*, 2101−2107.
[2] R. Driver, W. R. Walker, *Aust. J. Chem.* **1968**, *21*, 331−337.
[3] M. E. Bridson, W. R. Walker, *Aust. J. Chem.* **1970**, *23*, 1191−1197.
[4] G. C. Pappalardo, A. Seminara, *J. Inorg. Nucl. Chem.* **1976**, *38*, 1993−1995.
[5] A. Forchioni, V. Librando, G. C. Pappalardo, *J. Chem. Soc., Dalton Trans.* **1977**, 638−641.
[6] M. Kondo, S. Kawata, S. Kitagawa, H. Kiso, M. Munukata, *Acta Crystallogr., Sect. C* **1995**, *51*, 567−569.
[7] O. S. Jung, D. H. Jo, Y. A. Lee, B. J. Conklin, C. G. Pierpoint, *Inorg. Chem.* **1997**, *36*, 19−24.
[8] F. Nicolò, G. Bruno, G. Tresoldi, *Acta Crystallogr., Sect. C* **1996**, *52*, 2188−2191.
[9] G. Tresoldi, S. Lo Schiavo, P. Piraino, *Inorg. Chim. Acta* **1997**, *254*, 381−385.
[10] G. Tresoldi, E. Rotondo, P. Piraino, M. Lanfranchi, A. Tiripicchio, *Inorg. Chim. Acta* **1992**, *194*, 233−241.
[11] G. De Munno, G. Bruno, E. Rotondo, G. Giordano, S. Lo Schiavo, P. Piraino, G. Tresoldi, *Inorg. Chim. Acta* **1993**, *208*, 67−75.
[12] G. Tresoldi, P. Piraino, E. Rotondo, F. Faraone, *J. Chem. Soc., Dalton Trans.* **1991**, 425−430.
[13] W. M. Teles, N. G. Fernandes, A. Abras, C. A. L. Filgueiras, *Trans. Met. Chem.* **1999**, *24*, 321−325.
[14] R. J. Andersen, P. J. Steel, *Acta Crystallogr., Sect. C* **1998**, *54*, 2188−2191.
[15] G. Bruno, F. Nicolò, S. Lo Schiavo, M. S. Sinicropi, G. Tresoldi, *J. Chem. Soc., Dalton Trans.* **1995**, 17−24.
[16] G. Tresoldi, S. Lo Schiavo, P. Piraino, P. Zanello, *J. Chem. Soc., Dalton Trans.* **1996**, 885−892.
[17] G. Bruno, F. Nicolò, G. Tresoldi, *Acta Crystallogr., Sect. C* **2000**, *56*, 282−283.
[18] G. Bruno, F. Nicolò, G. Tresoldi, S. Lanza, *Acta Crystallogr., Sect. C* **2002**, *58*, M56−M58.
[19] R. Scopelliti, G. Bruno, C. Donato, G. Tresoldi, *Inorg. Chim. Acta* **2001**, *313*, 43−55.
[20] G. Tresoldi, S. Lo Schiavo, S. Lanza, P. Cardiano, *Eur. J. Inorg. Chem.* **2002**, 181−191.
[21] Z. Wolnicka-Rutkowska, Z. Talik, *Pr. Nauk. Akad. Ekon. im. Oskara Langego Wroclawiu* **1982**, *191*, 151−161; *Chem. Abstr.* **1983**, *98*, 1258316.
[22] D. Cremer, J. A. Pople, *J. Am. Chem. Soc.* **1975**, *97*, 1354−1358.
[23] E. W. Abel, D. Ellis, K. G. Orrell, *J. Chem. Soc., Dalton Trans.* **1992**, 2243−2249.
[24] E. W. Abel, P. J. Heard, K. G. Orrell, M. B. Hursthouse, M. A. Mazid, *J. Chem. Soc., Dalton Trans.* **1993**, 3795−3801.
[25] C. Chachaty, C. Pappalardo, C. G. Scarlata, *J. Chem. Soc., Perkin Trans. 2* **1976**, 1234−1238.
[26] F. Haviv, R. W. DeNet, R. J. Michaels, J. D. Ratajczyk, G. W. Carter, P. R. Young, *J. Med. Chem.* **1983**, *26*, 218−222.
[27] R. Diamond, *Acta Crystallogr., Sect. A* **1969**, *25*, 43−55.
[28] G. Kopfmann, R. Huber, *Acta Crystallogr., Sect. A* **1968**, *24*, 348−351.
[29] *XSCANS*, release 2.31, Bruker AXS Inc., Madison, Wisconsin, USA, **1999**.
[30] G. M. Sheldrick, *SHELXTL*, VMS version 5.05, Siemens Analytical X-ray Instruments Inc., Madison, Wisconsin, USA, **1991**.
[31] A. Altomare, O. Cascarano, C. Giacovazzo, A. Guagliardi, M. C. Burla, G. Polidori, M. Camalli, *J. Appl. Crystallogr.* **1994**, *27*, 435−436.
[32] G. M. Sheldrick, *SHELXL-97, Program for Crystal Structure Refinement*, University of Göttingen, Germany, **1997**.
[33] M. Nardelli, *J. Appl. Chem.* **1995**, *28*, 659; locally modified version.

Received February 13, 2004
Early View Article
Published Online June 7, 2004

